International Publication Awards

Tanta University

January - June 2010

Contents

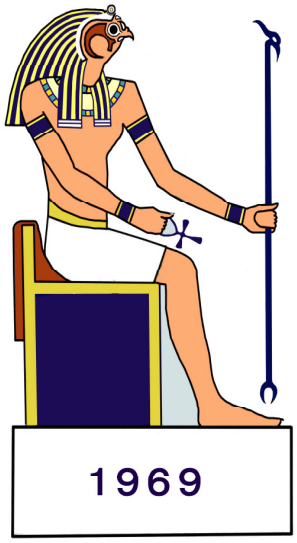

Faculty of Science

1- Molecular manipulation and modification of the genes encoding the G2 and G4 glycinin subunits.

Reda H. Sammour

Genetics and Molecular Biology, 29 (2006) 543-550.

Abstract

The genes encoding the glycinin subunits G2 and G4 were molecularly manipulated and modified to test the possibility of increasing the nutritional value of soybean seed proteins. The recombinant DNAs pSP65/G2HG4, pSP65/G4HG2, pSP65/248 Metl, pSP65/248 Met2,3 and pSP65/248 Metl.2,3 were used in in vitro translation to produce (i) chimeric proteins consisting of reciprocally exchanged acidic and basic G2 and G4 domains and (ii) Gy4 point mutants with an increased number of methionine residues. The ability of the recombinant proteins to assemble into proper quaternary structures was investigated using sucrose gradient fractionation. The data produced by this study could provide valuable clues for the potential improvement of genetically modified crops.

Keywords: *DNA, glycinin subunit G4, in vitro translation, mutagenesis, soybean.*

2- Nonlinear Kelvin Helmholtz Instability of magnetized surface waves on a subsonic gas–viscous potential liquid interface.

Magdy Mohamed Ali Sirwah,

Physica A, 375 (2007) 381–400.

Abstract

A nonlinear stability analysis, of magnetic fluids, was carried out for interfacial waves between a subsonic inviscid gas and viscous streaming liquid when a normal constant magnetic field is present. The viscosity term in the problem was carried out using the viscous potential theory. The nonlinear analysis results nonlinear partial differential equations, for different cases, using multiple scales method. Using the modulation concept, we have discussed different numerical examples to show the effects of the system parameters on criteria of the interfacial waves (in) stability.

Keywords: *Viscous potential theory; Sideband instability; Super-harmonic instability*

3- Engineering two mutants of cDNA-encoding Gy2 subunit of soybean glycinin capable of self-assembly in vitro and rich in methionine.

Reda H. Sammour

Biologia, Bratislava Section Cellular and Molecular Biology, 62 (2007) 394-399

Abstract

The main goal of this work was to make the cDNA-encoding subunit Gy2 of soybean glycinin, capable of selfassembly in vitro and rich in methionine residues. Two mutants (pSP65/G4SacG2 and pSP65/G4SacG2HG4) were therefore constructed. The constructed mutants were successfully assembled in vitro into oligomers similar to those occurred in the seed. The successful self-assembly was due to the introduction of Sac fragment of Gy4 (the codons of the first 21 amino acid residues), which reported to be the key element in self-assembly into trimers. The mutant pSP65/G4SacG2HG4 included the acidic chain of Gy4 (HG4), which was previously molecularly modified to have three methionine residues. This mutant will be useful in the efforts to improve the seed quality.

Key words: *soybean; Gy2; glycinin; self-assembly; G2 subunit.*

4- Electrical conductivity of silver bis muth borate tellurite glasses.

Mohamed Hany Ahmed Fouad Shaaban and Ali Abd El Hammed Ali.

Physica B 403 (2008) 2461–2467.

Abstract

The AC electrical conductivity of $(Ag_2O)x$ $(Bi_2O_3)30$ $(B_2O_3)60$ - x $(TeO_2)10$ glass (x = 0, 2, 4, 5, 10, 15 and 20) were measured at different temperatures and frequencies. The results obtained indicated that glasses containing silver 5 mol% have values nearly approximately equal to AC electrical conductivity. A slight decrease was observed with increasing Ag_2O concentration up to 4 mol%. However, the AC electrical conductivity values increase with increasing silver content, i.e. X5 mol %. The AC electrical conductivity values, increased with increasing frequency and follow the power law, $\sigma AC = A\omega s$. The frequency exponent s was found to be dependent on frequency and temperature. The s values tended to increase to unity as the temperature decreased. Such results suggest that the correlated barrierhopping (CBH) model is appropriate for explaining the AC electrical conductivity in these glasses. A pronounced increase in the dielectric loss values was observed with increasing silver content. These reflect the effect of Ag^+ ions charge carriers on the electrical conductivity of such glasses.

Keywords: *Conductivity; Silver bismuth borate tellurite; Glasses*

5- Non-Linear temporal dynamics of tow- mode interactions of magnetized flow.

Magdy Mohamed Ali Sirwah,

International Journal of Non-Linear Mechanics , 43 (2008) 416-436

Abstract

This paper considers, in the frame work of the model of two superposed layers of viscous-potential incompressible magnetic fluids, theproblem on formation of resonant waves of two modes on the interface between fluids that arisen as a result of second-harmonic resonance. The fluids moving with uniform velocities parallel to their interface are stressed by a tangential magnetic field. The analysis includes the linear, as well as the non-linear effects where the analytical solutions are constructed using the method of multiple scales, in both space and time, and hence the solvability conditions correspond to the uniform (convergent) solutions are obtained. The solvability conditions are then exploited to derive a more general system of non-linear partial differential equations with complex coefficients governing the amplitudes of the resonant waves. These equations are examined for solutions corresponding to sinusoidal wavetrains consequently different kinds of instabilities are demonstrated. The stability criterion in each case is derived and discussed both analytically and graphically.

Keywords: *Magnetic fluids; Resonant waves interaction; Non-linear Kelvin–Helmholtz instability*

6-4-[(3-Formyl-4-hydroxyphenyl)diazenyl)-N-(pyrimidin-2-yl) benzenesulfonamide.

Huda A. Al Gamry, Rafaat M. Issa, Kamal Y. El- Baradie, Keiko I. Masaoka and Ken Sakai

Journal of Acta Crystallographica Section, E, 65, (2008) 1673.

Abstract

The title molecule, $C_{17}H_{13}N_5O_4S$, has a Trans configuration with respect to the diazenyl (azo) group. The pyrimidine ring and the terminal benzene ring are inclined at angles of 89.38 (4) and 1.6 (6), respectively, with respect to the central benzene ring. The conformation of the molecule is in part stabilized by an intramolecular O—H---O hydrogen bond. In the crystal structure, molecules related through inversion centers form hydrogen-bonded dimers involving the sulfonamide N—H group and the N atom of the pyrimidine ring.

Keywords: *single-crystal X-ray study; T = 100 K; mean _(C–C) = 0.002 A°; R factor = 0.035; wR factor = 0.098; data-to-parameter ratio = 14.5.*

7- 1-[4-(Diaminomethyleneaminosulfony) phenylimin omethyl) -2 naphtholate N,N- dimethylformamide disolvate.

Huda A. Al Gamry, Rafaat M. Issa, Kamal Y. El- Baradie, Keiko Isagai, S. Masaoka and Ken Sakai

Journal of Acta Crystallographica Section), E, 64 (2008) 1350.

Abstract

The asymmetric unit the title compound, $C_{18}H_{16}N_4O_3S$- $2C_3H_7NO$, contains a molecule in a zwitterionic form with a deprotonated hydroxyl group and an iminium group, and two dimethylformamide solvent molecules. The dihedral angles of the guanidine group and the naphthyl ring system with respect to the central benzene ring are 76.04 (7) and 3.45 (9), respectively. The conformation of the molecule may be influenced, in part, by two intramolecular hydrogen bonds, while in the crystal structure, intermolecular hydrogen bonds form one-dimensional chains along [010].

Keywords: *single-crystal X-ray study; T = 100 K; mean _(C–C) = 0.003 A°; R factor = 0.037; wR factor = 0.091; data-to-parameter ratio = 16.6.*

8- The 844 Ma Moneiga quartz-diorites of the Sinai, Egypt: Evidence for Andean-type arc or rift-related magmatism in the Arabian-Nubian Shield

F. Bea, M. Abu-Anbar, P. Montero, P. Peres and C. Talavera.

Precambrian Research, 175 (2009) 161-168.

Abstract

U-Pb ion-microprobe zircon dating of the Moneiga quartz-diorites, located within the Katherine ring-complex of the Sinai, reveals a crystallization age of 844±4Ma and the presence of 1045Ma premagmatic zircon cores. These rocks are much older than previously believed, and represent the oldest magmatic rocks so far dated in the Sinai. Their chemical composition corresponds to mildly silicic, low- to medium-K, metaluminous, calcic to calc alkaline rocks with somewhat elevated FeOtotal/MgO, low Ba/La and high Cs/Sc and Zr/Yb. The initial Sr and Nd isotope composition (86Sr/87Sr844Ma = 0.703187±0.000034 and _Nd844Ma 3.5±0.5) is slightly less primitive than expected from similar rocks of Arabian-Nubian Shield with the same age. Trace-element and isotope ratios reveal the presence of a non-juvenile crustal component that caused a TDM = 1.06±0.06 Ga identical to the age of the oldest pre-magmatic cores of zircons. These data support the idea that the Moneiga quartz-diorites formed by re-melting of a 200Ma old island-arc crust during the early stages of the prolonged break-up process of Rodinia.

Keywords: *Sinai, Rodinia, Mozambique Ocean, Continental rifting, Zircon inheritance*

9- Electrochemical and SEM properties of Co^{2+} ion hexagonal mesophase of pluronic lyotropic liquid crystal template.

Ibrahim Shibl El-halag,

Bull. Mater.Sci ,132 (2009) 555–560 .

Abstract

The electrochemical and SEM properties of Co^{2+} ion in hexagonal mesophase of the pluronic lyotropic liquid crystal template are reported. The cyclic voltammetric studies evidenced the occurrence of two slow electron transfer reduction processes. Such a reaction presumably related to the reduction of Co^{2+} ion to Co metal. The hexagonal (H1) lyotropic liquid crystalline phases of P84 surfactant have been used to template the electrochemical deposition of nanostructured cobalt films as well as its uses as background electrolyte. Electrochemical studies show that these films have very high surface areas, which reveals that the deposited film exhibits promising properties. The electrode parameters of Co(II) ion in hexagonal meso phase of the lyotropic liquid crystal ternary system (pluronic P84/cobalt/p-xylene) is determined using cyclic voltammetry, deduced convolutive voltammetry and chronoamperometry techniques. The morphology of nanostructured deposited films of Co^{2+} ion in pluronic lyotropic liquid crystal template was investigated via scanning electron microscopy (SEM) technique.

Keywords: *Electrochemical properties; hexagonal mesophase; liquid crystal; deduced convolutive voltammetry; chronoamperometry*

10- Theoretical investigation of the inhibition of corrosion by some triazole Schiff bases.

Mohamed Khaled Awad, Rafaat Mustafa Issa and Fatten Mahmoud Atlam,

Materials and Corrosion, 60 (2009) 813–819.

Abstract

An examination of quantum chemical and corrosion inhibition studies is carried out to investigate whether any clear links exist between the results of quantum chemical calculations and the experimental inhibition efficiencies.The influence of the investigated triazole Schiff bases, (benzylidine amino) triazole (a), 4-hydroxy 3-(benzylidine amino) triazole (b), 2-hydroxy 3-(benzylidine amino) triazole (c), and 2- hydroxy 3-(naphthylidine amino) triazole (d) on the inhibition of corrosion of the metal surfaces are studied by density functional theory at the B3LYP/6-31G level. The calculated quantum chemical parameters correlated to the inhibition efficiency are, the highest occupied molecular orbital (HOMO), the lowest unoccupied molecular orbital (LUMO), the separation energy (DE), the dipole moment (m), the softness (s), the total negative charge on the whole molecule (TNC), the total charge on the azo-methine moiety, the molecular volume (Vi), and the total energy (TE). A good correlation between the quantum chemical parameters and the experimental inhibition efficiency is found. High inhibition efficiency for corrosion inhibitors can be achieved by controlling their electronic and structural properties.

Keywords: *DFT calculation, Schiff bases, Corrosion inhibitors*

11- Instability analysis of resonant standing waves in a parametrically excited boxed basin.

Magdy Mohamed Ali Sirwah

Physica Scripta 79,(2009) 065404,(23pp).

Abstract

Two-mode parametric excited interfacial waves of incompressible immiscible liquids in an infinite boxed basin subjected to a vertical excitation are studied. The method of multiple time scales is used to obtain uniform solutions of the second-order system as well as the third-order one, which in turn leads to the solvability conditions of the two orders including the cubic interaction terms. The different cases of resonance that arise among the natural frequencies together with the frequency of the vertical vibration of the box are demonstrated theoretically and numerical computations of one of these cases (the two-to-one internal resonance and the principal parametric resonance) have been performed in detail in order to investigate the behavior of the resonant waves, especially the qualitative one. The autonomous system of four first-order differential equations for the modulation of the amplitudes and phases of the resonant waves is derived. Some numerical applications are achieved to show the stability criteria of the excited liquids inside the considered basin.

Keywords: *Parametric instability; Standing waves; Bxed basin; Chaotic Motion*

12- Dibromido (2,3,9,10- tetramethy l-1,4,8,11-tetraazacyclotetradeca 1,3,8,10- tetraene) cobalt(lll) bromide.

Huda Abu Al Futoh Al-Gamry, Rafaat Mostafa Issa, Kamal Yosuf El- Baradie, S. Masaoka andKen Sakai

Journal of Acta Crystallographica Section, E, 65 (2009) , 1378.

Abstract

In the title compound, $[CoBr_2(C_{14}H_{24}N_4)]Br$, the Co(III) ion is located on an inversion centre and possesses a distorted octahedral coordination geometry in which four nitrogen donors of the ligand molecule are in the equatorial plane and two Br^- ions occupy both the axial sites to give a trans isomer. The Br^- counter- anion is also located on an inversion centre.

Keywords: *single-crystal X-ray study; T = 100 K; mean _(C–C) = 0.002 A°; R factor = 0.016; wR factor = 0.040; data-to-parameter ratio = 16.7.*

13- Simple Method for Stationary Organotypic Slice Culture of Hypothalamic Suprachiasmatic Nucleus.

Ehab Mostafa Tousson,

Journal of Neurological Sciences (Turkish), 26(4) (2009), 442–449.

Abstract

Early postnatal brain tissue can be cultured in viable and healthy condition for several weeks with development and preservation of the basic cellular and connective organization as so-called organotypic brain slice cultures. The present study describes a simple method for stationary long-term organotypic culture for the hypothalamic suprachiasmatic nucleus (SCN). Hypothalamic brain slices from 1-12 day old mice were maintained in culture at the interface between air and culture medium. These slices were supported by Millicell filters without need for any strategies to promote adherence and incubated in Petri dishes. This model of organotypic slice culture was characterized by the simplicity of handling, high yields of viable and thin slices which remain 1-3 cell layers thick. It can be used to make organotypic slices from a range of ages, other parts of the brain and other rodent species.

Keywords: *organotypic slice culture, hypothalamus, suprachiasmatic nucleus, development, immunohistochemistry, mouse*

14- Dielectric Properties Investigation of Polyaniline Prepared by Using Fentons Reagent.

Mohamed M. Ayad, E. Zaki and Mustafa Al Nmr

International Journal of Polymer Analysis and characterization, 14 (2009) 652–665.

Abstract

The frequency dependence of the dielectric properties and dc conductivity (σ_{dc}), of polyaniline samples that have been prepared in a conducting state by a chemical method using Fenton reagent, were investigated. These samples were prepared at constant molar ratio H_2O_2/aniline (r =1) and at different concentrations of both H_2O_2 and aniline (0.2 M, 0.4 M and 0.5 M). The measurements were carried out using the complex impedance technique in frequency range (0.12 to 100 KHz) at temperature range from about 278 K to 311 K. It has been found that the concentrations of H_2O_2 and aniline have a noticeable effect on the dielectric properties. All samples have only one activation energy for one phase of material except at 0.5 M implying several activation energies and consequently several phases in the material.

Keywords: *Fenton regent, Polyaniline, Dielectric properties*.

15- Stripping Voltammetric Methods for determination the antiparasitic drug nitazoxanide in bulk from, pharmaceutical formulation and human serum

Mohamed M. Ghoneim, Hana S. Al Dosoky and Mohamed M. Abd Al Galel

Journal of Brazilian Chemical Society, 20, 1 (2009)

Abstract

Cyclic voltammograms of nitazoxanide recorded at the hanging mercury drop electrode in the Britton-Robinson universal buffer of pH values 2 to 11 containing 20% (v/v) ethanol exhibited a single 4-electron irreversible cathodic peak corresponding to the reduction of its NO_2 group to the hydroxylamine stage. Nitazoxanide was found to adsorb onto surface of the mercury electrode in a monolayer surface coverage of 3.16×10^{-10} mol cm^{-2} in which each adsorbed molecule occupies an area of 0.525 nm^2. Based on its adsorption behavior onto the mercury electrode surface, validated linear sweep (LS), differential pulse (DP) and square wave (SW) adsorptive cathodic stripping voltammetric methods were described for determination of bulk nitazoxanide. Limits of detection of 1.5×10^{-10}, 2.4×10^{-10} and 3.0×10^{-11} mol L^{-1} and limits of quantification of 5.0×10^{-10}, 8.0×10^{-10} and 1.0×10^{-10} mol L^{-1} nitazoxanide in the bulk form were achieved by means of the described LS, DP and SW adsorptive cathodic stripping voltammetric methods, respectively. The described methods were successfully applied for determination of nitazoxanide in its pharmaceutical formulation (Cryptonaz powder) and in spiked human serum without the necessity for sample pretreatment, time consuming extraction steps or formation of colored chromogens prior to the analysis. Besides, nitazoxanide was successfully determined without interference from its acid or base-induced degradation products indicating the stability-indicating power of the described voltammetric methods.

Keywords: *Nitazoxanide; Cryptonaz powder; Human serum, Degradation, Determination; stripping voltammetry*

16- Reduction of the dimensionality and comparative radiological data.

M.K.Sedeek, M.Abd El-Manam Kozae, Taher M. Sharshar and Husan M. Badran,

Applied Radiation and Isotopes, 67 (2009) 1721–1728.

Abstract

Computational methods were used to reduce the dimensionality and to find clusters of multivariate data. The variables were the natural radioactivity contents and the texture characteristics of sand samples. The application of discriminate analysis revealed that samples with high negative values of the former score have the highest contamination with black sand. Principal component analysis (PCA) revealed that radioactivity concentrations alone are sufficient for the classification. Rough set analysis (RSA) showed that the concentration of 238U, 226Ra or 232Th, combined with the concentration of 40K, can specify the clusters and characteristics of the sand. Both PCA and RSA show that 238U, 226Ra and 232Th behave similarly. RSA revealed that one or two of them can be omitted without degrading predictions.

Keywords: *Computational methods, Principal Component analysis, Rough Set analysis*

17- Geology and petrogenesis of Neoproterozoic migmatitic rock astern Desert, Egypt Implications for syntectonic anatectic migmatites.

Gafar Abd El Alem Al Bhrayh,

Lithos, 113 (2009) 465–482.

Abstract

Detailed field geology and mapping, field observations, structural and metamorphic criteria, petrographic description and mineral chemistry have been used to investigate the geology and petrogenesis of Neoproterozoic genetically related migmatitic rocks in the Hafafit region of the Eastern Desert of Egypt. Diatexites and schlieric granites occupy the core of the regional domal structure and are flanked by metatexites and preserved metagabbros and amphibolites. Metatexites are composed of migmatitic amphibolites, diatexites include mainly migmatitic gneisses and schlieric granites comprise gneissic tonalites, geissic granodiorites, together with subordinate gneissic trondhjemites. Mylonitic gneisses occur along local shear zones. This migmatitic association was intruded later by syenogranite. The rocks have experienced three deformational events (D1–D3) contemporaneous with three metamorphic phases (M1–M3). An early medium pressure–high temperature prograde metamorphism (M1) during regional-scale deformation (D1) leads to migmatization under water-rich conditions of upper amphibolites facies. Dynamothermal metamorphism (M2) was contemporaneous with D2 and confined to the diapiric uplift of the anatectic solid–melt mixture in the core of the dome. D1 and D2 events pertain to a single orogeny during crustal shortening and represented the most pervasive fabric in the study area. Plagioclase, clinopyroxene, hornblende, garnet and biotite showcompositional variability as a consequence of the composition of protoliths, prevailing P–T conditions of metamorphism and variable degrees of partial melting, back reaction and crystallization of residualmelt. The earliermineralphases inmetatexites are enriched inMg and Ca and depleted in Fe, Mn and Na relative to the refractory minerals in diatexites and schlieric granites. Hornblende, garnet and biotite occur as xenocrysts in syenogranite and are enriched in Na, Fe, andMn relative to those in the migmatitic rock association. Thermobarometry based on element partitioning between coexisting minerals indicates that peak metamorphism and partial melting occurred at ~750 °C and ~5 kb at high H_2O activity for the metatexite. The obtained P–T conditions indicate a clockwise P–T path. The migmatitic rock association appears to have been generated by variable degrees of water-saturated partial melting of arc-related gabbroic and amphibolitic rocks at medium pressure and high temperature. Diatexites and schlieric granites occur in structurally controlled sites suggesting syntectonic melt flow within and through the migmatites.

Syntectonic anatectic migmatization occurred under a compressional regime and was followed by diapiric emplacement of anatectic melt in the same setting. The rocks thus provide an example of the close relation between metamorphism, deformation, and melt generation and emplacement. The present rock association is interpreted as syntectonic anatectic migmatites and granitoid intrusives of Pan-African orogeny during the formation of an Andean-type continental margin.

Keywords: *Neoproterozoic migmatitic rock, astern desert, metamorphism, deformation*

18- Stability Indicating Square-wave Stripping Voltammetric Method for Determination of Gatifloxacin in Pharmaceutical Formulation and Human Blood,

Hanaa Salah El-Desoky,

J. Braz. Chem. Soc.,20(10) 1790 (2009)

Abstract

A fully validated, sensitive and precise stability-indicating square-wave adsorptive cathodic stripping voltammetric method has been developed for determination of gatifloxacin in the bulk form, pharmaceutical formulation, and in spiked human serum and real plasma samples. The achieved detection limits of gatifloxacin in the bulk form and human serum were 1.5×10^{-9} and 2.2×10^{-9} mol L^{-1}, respectively. The described method was applied successfully for determination of gatifloxacin in formulation and human biological samples without extraction prior to the analysis. No significant interferences from common excipients, some common metal ions, organic species, co-administrated drugs and from the acid-induced degradation product were obtained during analysis of gatifloxacin in the various analyzed samples. Besides, pharmacokinetic parameters of gatifloxacin in plasma of healthy volunteers following the administration of an oral single dose (400 mg gatifloxacin) were also estimated by means of the described stripping voltammetric method.

Keywords: *Gatifloxacin; Tequin tablets; Human blood; Stripping voltammetry; Pharmacokinetic parameters*

19- Electrochemical Oxidation of Iodide a at Glassy Carbon Electrode in Methylene Chlorige at Various Temperatures.

Ibrahim Shibl El-halag.

J. Chil. Chem Soc., 54 (2010) 331– 337 .

Abstract

Anodic electrooxidation of iodide in 0.1 mol L^{-1} TBAP/CH_2Cl_2 was studied electrochemically via cyclic voltammetry, convolution transforms voltammetry, chronoamperometry and chronopotentiometry techniques at a glassy carbon electrode (GCE) at various temperature ranging from -20 ^oC to 21 ^oC . It was found that at less positive potential triiodide (I^{-3}) is formed followed by a moderate fast chemical process, while at more positive potential, the triiodide is oxidized to iodine (I_2) followed by another chemical process, i.e EC_1EC_2 scheme. The effect of lowering the temperature on the heterogeneous electron transfer rate constant and the diffusion coefficient was discussed. The relevant chemical and electrochemical parameters of the electrode reaction were determined. The accurate test of the parameters evaluated experimentally was verified by comparing the experimental voltammograms with the simulated on .

Keywords: *Convolution transforms voltammetry, electrochemical parameters, digital simulation, chronoamperometry, chronopotentiometry*.

20- Synthesis, characterization and biological activity studies of copper (II) metal(II) binuclear complexes of dipyridylglyoxal bis (2-hydroxybenzoyl hydrazone).

Ali El Dosoky, Othman Al-Fulaij, Bakir Jeragh, Mohamed Khaled Awad and Sayed Rizk,

Journal of Coordination Chemistry, 63 (2) (2010) 330–345.

Abstract

A new series of copper (II) mononuclear and copper(II)-metal(II) binuclear complexes of the formula $[(H_2L)Cu].H_2O$, $[CuLM].nH_2O$and $[Cu(H_2L)M(OAc)_2].nH_2O$, n = 1-2, M = Co(II), Ni(II), Cu(II) or Zn(II) and L is the anion of dipyridylglyoxal bis(2-hydroxybenzoyl hydrazone), H_4L, were synthesized and characterized. The elemental analyses, molar conductivity values and FT-IR spectra supported the formulation of these complexes. The IR data suggests that H_4L acts as a dibasic tetradentate in $[(H_2L)Cu].H_2O$ and $[Cu(H_2L)M(OAc)_2].nH_2O$ but tetra-basic hexadentate in $[CuLM].nH_2O$, n = 1- 2. Thermal studies indicate that the water molecules are of crystallization and the complexes are thermally stable up to 347 – 402 ^oC depending upon the nature of the complex. The thermal decomposition steps are given. The magnetic moment values at room temperature and/or at different temperatures indicate the presence of a magnetic exchange interaction between Cu(II) and M(II) centers in the binuclear complexes. The electronic spectral data show that the energy of the d-d transitions of CuN_2O_2 in the mononuclear complex are blue shifted in the binuclear complexes in the sequences: Cu-Cu > Cu-Ni > Cu-Co > Cu-Zn suggesting that the binuclear complexes $[CuLM].nH_2O$ are more planar than the mononuclear complex. The structure of complexes was energetically optimized through molecular mechanics applying MM^+ force field coupled with molecular dynamics simulation The complexes $[(H_2L)Cu].nH_2O$ and $[CuLM].nH_2O$ and the free ligand were screened for their antimicrobial activities on some Gram-positive and Gram-negative bacterial species. The free organic ligand is found to be inactive against all studied bacteria. The complexes $[(H_2L)$ Cu$].H_2O$ and $[CuLCu].H_2O$ are found the most active with wide spectra. The screening data showed that $[CuLCu].H_2O$ > [(H2L) Cu$].H_2O$ > $[CuLZn].H_2O$ > $[CuLNi].2H_2O$ ≈ $[CuLCo].H_2O$ in order of increasing biological activity. The data are discussed in terms of their compositions and structures.

Keywords: *2,2'-pyridil, homo- and hetero-binuclear complexes, spectra, magnetism, biological activity*

21- Metabolic consequences of chronic sublethal ammonia exposure at cellular and subcellular Levels in Nile tilapia brain.

Mona Abd El Manam Hagazi, Zainab Ibrahim Ali Attia, Mohamed Abd El Manam Hagazi and Soha Sameh,

Aquaculture, 299(1-4) (2010) 149–156.

Abstract

The objective of this study was to elucidate the mechanism of chronic sublethal ammonia exposure in the brain of Nile tilapia, Oreochromis niloticus, by examining the cytosolic (c) and mitochondrial (m) enzymes related to ammonia detoxification. The experiment was conducted for 70 days on the juveniles of Nile tilapia (18±2.1 g) exposed to the total ammonia nitrogen concentration (TAN) of 5 (LL) or 10 (HH) mg L^{-1} in a static water system at 26°C. The activities of c-alanine aminotransferase (c-ALT), c-aspartate aminotransferase (c-AST), c-malic enzyme (c-ME), m-malic enzyme (m-ME), glutamate dehydrogenase (GDH) in the amination direction, and glutamine synthetase (GSase) in fish exposed to one of these sublethal TAN concentrations were significantly increased. The increase in the enzyme activity was positively related to the level of the tested TAN concentration. However, the activity of m-ALT and glutaminase (GLase) was significantly decreased, and that of m-AST did not show any significant changes. On the other hand, in Nile tilapia exposed to HH, there was a significant increase in the levels of free amino acids (FAAs), such as alanine, glutamine, glycine, histidine, serine, and γ-aminobutyric acid (GABA); however, no alteration in asparagine was observed, and there was a significant decrease in the levels of aspartate and glutamate. The significant increase in FAAs levels in fish exposed to LL was mainly attributable to alanine, glutamine, and GABA, and the importance of these metabolic changes in the cytosolic and mitochondrial ALT, AST, and ME was discussed.

Keywords: *glutamine, glutamate, aspartate, GABA, alanine, cytosolic and mitochondrial ammonia detoxification enzymes.*

22- Spectral behavior and laser activity of 3-(4-dimethylaminopheny1)-1-(h-pyrrol-2-yl) prop-2-en-1-one (DMAPRP). A new laser dye.

Yusif Sobhy El-Sayed, Mohamed Gaber and Samy Abd Allah Al- Daly

Optics and Laser Technology , 42 (2010) 397– 402.

Abstract

The photophysical properties of DMAPrP have been investigated in different solvents. DMAPrP dye exhibits a large change in dipole-moment upon excitation due to an intramolecular charge transfer interaction. A crystalline solid of DMAPrP give an excimer like emission at 546 nm. The ground and excited state protonation constants of DMAPrP are calculated. DMAPrP acts as good laser dye upon pumping with nitrogen laser in some organic solvents. The laser parameters such as the tuning range, gain coefficient (a), emission cross section (σe) and half-life energy ($E_{1/2}$) are also calculated. The photoreactivity and net photochemical quantum yield of DMAPrP in chloromethane solvents are also studied.

Keywords: *Chalcones; Effect of solvent polarity; Laser dye.*

23- Effects of chronic exposure to ammonia concentrations onbrain monoamines and A TPases of Nile tilapia (Oreochromis niloticus).

Mona Abd El Manam Hagazi and Soha Sameh Hasanein,

Comparative Biochemistry and Physiology, Part C, (2010).

Abstract

The effects of chronic exposure to total ammonia nitrogen (TAN) concentrations on the brain monoamines and ATPases of Nile tilapia, Oreochromis niloticus fingerlings, were studied. The period of exposure was 70 consecutive days, and the initial weight of the fingerlings was 18 ± 2.1 g. In addition to the control, three treatment groups exposed to 2.5 (low), 5 (medium), and 10 (high) mg TAN L^{-1} concentrations were tested. The unionized ammonia nitrogen (NH_3) levels calculated in mg L^{-1} were 0.059, 0.185, and 0.575 in aquaria at 26 °C. The brain monoamines were serotonin (5-HT), dopamine (DA), and norepinephrine (NE), as well as their derivatives, 5-hydroxyindoleacetic acid (5-HIAA) and dihydroxyphenylacetic acid (DOPAC). Compared with the controls, the levels of brain monoamines and Na^+/K^+- and Ca^{2+}-ATPase activities were not significantly altered in fish exposed to low TAN concentration. However, there was a significant decrease in 5-HT, DA, and NE levels, and a significant increase in both serotonergic (5-HIAA/5-HT) and dopaminergic (DOPAC/DA) activities of fish exposed to medium TAN and high TAN concentrations. The activities of brain Na^+/K^+- and Ca^{2+}-ATPase of fish exposed to medium TAN and high TAN concentrations significantly increased, while Mg^{2+}-ATPase did not significantly change compared with that of the controls. The quantity of the detected alterations increased in fish exposed to high TAN concentration.

Keywords: *Growth rate; Plasma ammonia; Na^+/K^+- and Ca^{2+}-ATPase, Mg^{2+}-ATPase; Serotonin; Dopamine; Norepinephrine; 5-hydroxyindoleacetic acid (5-HIAA); Dihydroxyphenylacetic acid (DOPAC)*

24- Eological status of the Mediterranean juniperus phoenicea L. Relicts in the desert mountains of North Sinai, Egypt.

Kamal H. Shaltot, Magde I. Al Bana, Ahmed H. Allah and Husny A. Musalam,

Flora ,205 (2010) 171–178.

Abstract

Juniperus phoenicea L. is listed as threatened tree by IUCN Red List. In Egypt, Juniperus phoenicea L. is the only conifer tree that is restricted to the three mountains of northern Sinai: Gabal El-Halal, Gabal El-Maghara and Gabal Yelleq. It has been included in a national list as a Mediterranean relicts target for conservation and management. To provide baseline information for the development of a conservation strategy, the present study aims at comparing the isolated populations of J. phoenicea and their associated plant composition and diversity at the three mountains. The application of TWINSPAN and DCA analysis techniques has resulted in the identifying of four vegetation types associated with juniper, and each could be related to a specific geomorphologic habitat on a topographic gradient. Chiliadenus montanus and Zygophyllum dumosum characterized the slopes of smooth-faced rock outcrops in Wadi Abu Seyal (at 350 – 470 m belt of Gabal El-Halal), Deverra tortusa, Ephedra aphylla and Gymnocarpos decander inhabited the soil pockets of north-facing slope in Neqeb Abu Hamam (at 600 – 700 m belt of Gabal El-Halal), Stachys aegyptiaca and Moricandia nitens occupied the runnels of Wadi Arar (at 450 - 560 m belt of Gabal El-Maghara), and Artemisia herba-alba, Atriplex halimus and Reaumuria hirtella represent the stands on slope runnels (at 900 – 960 m) of Gabal Yelleq. The two groups recognized at Gabal El-Halal had, on average, the highest species diversity, and juniper density and cover. Juniper is generally in poor conditions at higher elevation (600 – 960 m) with a higher proportions of old and recent dead trees, and with the predominance of male individuals at the populations of Gabal El-Maghara and Gabal Yelleq. In contrast, the juniper populations at lower elevation (350-470 m) of Gabal El-Halal proved to be in best condition with mostly living foliage and reproductive branches. The differences in rock types and elevation among the three mountains reflect serious limitation on recruitment of J. phoenicea due to moisture availability. The results of this study showed that J. phoenicea is an endangered community and its conservation in northern Sinai Mountains is a priority. For the conservation of this community to be successful it would be necessary to preserve the suitable habitats at Gabal El-Halal.

Keywords: *Desert rocks, Juniperus phoenicea, conservation, North Sinai, size structure, tree vitality*

25- Oxidation of Levafix CA reactive azo- dyes industrial wastewater of textle dyeing by electro- generated fenton s reagent.

Hana Salah Al Dosoky, Mohamed M. Ghoneim, Raja El-Sheikh and N.M. idan

Journal of Hazardous Materials ,175 (2010) 858-865.

Abstract

The indirect electrochemical removal of pollutants from effluents has become an attractive method in recent years. Removal (decolorization and mineralization) of Levafix Blue CA and Levafix Red CA reactive Azo-dyes from aqueous media by electro-generated Fenton's reagent (Fe^{2+}/H_2O_2) using a reticulated vitreous carbon cathode and a platinum gauze anode was optimized. Progress of oxidation (decolorization and mineralization) of the investigated azo-dyes with time of electro-Fenton's reaction was monitored by UV–visible absorbance measurements, Chemical oxygen demand (COD) removal and HPLC analysis. The results indicated that the electro-Fenton's oxidation system is efficient for treatment of such types of reactive dyes. Oxidation of each of the investigated azo-dyes by electro-generated Fenton's reagent up to complete decolorization and approximately 90–95% mineralization was achieved. Moreover, the optimized electro-Fenton's oxidation was successfully applied for complete decolorization and approximately 85-90% mineralization of both azo-dyes in real industrial wastewater samples collected from textile dyeing house at El-Mahalla El-Kobra, Egypt.

Keywords: *Levafix blue and red reactive azo-dyes, Electro-Fenton's oxidation, Wastewater, Decolorization, Mineralization*

26- Self-assembly of coordination polymers constructed from CuCn and unidentate pyridine bases.

Safa El Den H. Atuo, Said Anwar Ismael and Mohamed M. Al Bendary.

Journal of Materials Science, 45 (2010) 1307–1314.

Abstract

The self-assembly of K3[Cu(CN)4] and unidentate pyridine bases (L): pyridine (py), 3-methyl pyridine (3-mpy) and 2,4,6-trimethyl pyridine (tmpy) in the presence of Me3SnCl affords new coordination polymers (CPs) CuCN.0.5(py)] (1), [CuCN.0.5(3-mpy)] (2) and [CuCN.0.5(tmpy)] (3). The syntheses are achieved in H2O/acetonitrile media at room temperature. The structure of the CP 3 was characterized by X-ray single crystal analysis. It is crystallized as orthorhombic in the space group Pnma, a = 9.1065 (3) Å, b = 8.6669 (3) Å and c = 12.1998 (5) Å and Z = 8. The CPs 1,2 were investigated by IR, mass, Uv-visible and ^{1}H-NMR spectra, as well as TGA. The CPs 1-3 are 2D-polymers consisting of 1D-(CuCN)n chain structure while the ligands alternate on both sides of the chain with associated copper atom coordination number of three. Hydrogen bonds play an essential role for developing 2D-network structure. These CPs exhibit strong fluorescent emissions in the solid state.

Keywords: *Coordination polymer, X-ray analysis, H-NMR spectra, Fluorescent emissions*

27- Synthesis and characterization of polyaniline – camphorsulphonic acid nanotube film,

Mohamed M. Ayad, N. Prastomo and A. Matsuda

Materials Letters, 64(3) (2010) 379–382.

Abstract

Polyaniline (PANI) nanotubes were prepared in the bulk solution and as films using the aniline oxidation with ammonium peroxydisulfate in aqueous solutions of camphorsulfonic acid (CSA). The in situ PANI films produced during the oxidation of aniline in CSA and also in hydrochloric acid solutions were followed by monitoring the frequency changes of quartz crystal microbalance (QCM). The kinetics of the film formation were discussed. The scanning electron microscopy (SEM) and scanning transmission electron microscopy (STEM) showed PANI nanotubes. In addition, nanorods and nanoflowers composed from nanofibers and nanoflakes are also present to some extent. The nanotubes were characterized using UV-Vis spectroscopy.

Keywords: *Polyaniline nanotube film; Camphorsulfonic acid; Quartz crystal microbalance.*

28- Sensing of silver ions by nanotubular polyaniline film deposited on quartz–crystal in a microbalance.

Mohamed M. Ayad, Prastomo, A. Matsuda and J. Stejskla

Synthetic Metals,160 (1-2) (2010) 42–46.

Abstract

Nanotubular polyaniline film was deposited onto the electrode of the quartz crystal microbalance (QCM). The film in the form of emeraldine base was exposed to a solution of silver nitrate. The reduction for silver ions took place and silver nanoparticles were produced at the film surface. The deposition of silver was monitored by using the QCM and the UV-visible spectroscopy. The morphology of the film before and after the silver deposition was studied by the scanning and transmission electron microscopy. Silver nanoparticles had sizes of about 50–120 nm and globular and triangular shape. X-ray diffraction and infrared spectroscopy were used to characterize the structure of the composite. The present approach could be used for noble-metal recovery in waste waters.

Keywords: *Quartz crystal microbalance; Polyaniline nanotubes; Silver;*

29- Effect of abiotic conditions on phragmites australis along geographic gradients in lake Burullus, Egypt.

Ibrahim M. Eid , Kamal H. Shaltot ,Yassen M. Al Sodane and Kay Yansen,

Aquatic Botany ,92 (2010) 86–92.

Abstract

Stand structure and biomass production of Phragmites australis (Cav.) Trin. ex Steud. were analyzed along north-south and east-west transects in the Burullus coastal lagoon (N Egypt, 410 km^2) at monthly intervals over a period of 1 year (February 2003 until January 2004). For this purpose, young and old stands were selected at eight different locations in the lagoon. It was found that the north-south transect mainly represented a fertility gradient (207-286 mg l^{-1} TN, 30-106 mg l^{-1} TP), while the east-west transect was associated with significantly decreasing salinity (7-4 ppt). All morphological and biomass variables of P. australis were significantly different between young and old stands. On average, the old (7.3 ± 0.2 kg DW m^{-2}) accumulated three times more total above-ground biomass than the young stands (2.5 ± 0.1 kg DW m^{-2}). Shoot height, diameter and shoot dry weight significantly increased by 25-50% with increasing fertility along the north-south transect. Shoot density significantly decreased from north to south, while it almost doubled in the north sites from 109 ± 6 to 216 ± 7 shoots m^{-2} along the west-east transect. In separate stepwise multiple regressions, variation in water quality explained 34-63% of the variation in morphology and total above-ground biomass in the old stands (salinity and water level were most important for biomass, transparency also for height and density) while it explained 16-42% of variation in young stands (mainly transparency).

Keywords: *Eutrophication, Nile Delta, Nutrient budget, Salinity gradient, Stand age, Total above-ground biomass, Water characteristics*

Faculty of Medicine

1- Sexual function among women with stress incontinence after using transobturator vaginal tape, and its correlation with patient's expectations.

Mohamed Abo Elnein Ghaloush, Maged Ragab, Abdel Nasser Al Gasmey, Osama Al Ashri, Mahmoud Al- Sharabi, Adel Al badri and Nahla Fayed.

British Journal of Urology International, 104 (2009) 1118-1123.

Abstracts

To evaluate changes in female sexual function after a transobturator vaginal tape (TOT) procedure for treating genuine stress urinary incontinence (SUI), and its correlation with patient's expectation.

PATIENTS AND METHODS The study included women treated with a suburethral TOT for genuine SUI, neurologically intact, heterosexual and married, aged 18 years, with no previous history of malignancy, pelvic radiotherapy and no other associated surgical or psychological diseases. Patients were interviewed before surgery and with the aid of a questionnaire including female sexual function, the Beck depression indices and their expectation of sexual function after surgery.

RESULTS: Sixty-two premenopausal sexually active women were included (mean age 40.5 years). The cure rate from SUI was 92%, 89%, 87% and 84% at 6, 12, 18 and 24 months, respectively. All patients attended the visit before and the first visit after surgery, while 71%, 42% and 24% were assessed at the 12-, 18 and 24-month visits, respectively. The mean follow-up was 12 months. Fifty two women resumed their sexual activity early within the 8 weeks after surgery and the frequency of coitus in more than two thirds of patients was at least once per month. The number of women who expected either looseness or tightness of the vagina was more than that estimated from patient perceptions. There was a difference between the patient's sensation of vaginal length abnormalities during coitus (two women) and patient expectation (18 women).

CONCLUSION: Although the TOT is effective for treating SUI, counseling the patient and her partner is important in correcting false ideas and expectations about future sexual activity. Indeed, sexual dysfunction is reported after vaginal surgery, with a physiological and psychological background. Further assessment should be used to characterize sexual dysfunction after vaginal surgery for SUI to find new solutions.

Keywords: *stress urinary incontinence, suburethral vaginal tape, transobturator tape, female sexual function*

2- An experimental study on ulcerative colitis as apotential target for probioctic therapy by Lactobacillus acidophilus with or without" olsalazine.

Amany Abdel Rahim Abdin and Eman Mohammed Ibraheim Said.

Journal of Crohn's and Colitis,2 (2008) 296-303.

Abstract

Traditional medical treatments for ulcerative colitis (UC) are still compromised by its adverse effects and not potent enough to keep in remission for long-termperiods. So, new therapies that are targeted at specific disease mechanisms have the potential to provide more effective and safe treatments for ulcerative colitis. Probiotics is recently introduced as a therapy for ulcerative colitis. In the present study, Lactobacillus acidophilus was selected as a probiotic therapy to investigate its effects in oxazolone-induced colitis model in rats that mimics the picture in human. The rats were grouped (8 rats each) as normal control group (Group I), Group II served as untreated oxazoloneinduced colitis, Group III oxazolone-induced colitis treated with probiotic L. acidophilus (1×10^7 colony-forming units (CFU)/mL/day oral for 14 days), Group IV oxazolone-induced colitis treated with olsalazine (60 mg/kg/day oral for 14 days), Group V oxazolone-induced colitis treated with probiotic L. acidophilus and olsalazine in the same doses and duration. Disease activity index (DAI) was recorded, serum levels of C-reactive protein (CRP), tumor necrosis factor-α (TNF-α) and intrleukin-6 (IL-6) was assessed as inflammatory markers and the histopathological picture of the colon of each rat was studied. Disease activity index (DAI) showed significant positive correlation with the elevated serum levels of CRP (r=0.741, pb0.05), TNF-α (r=0.802, pb0.05) and IL-6 (r=0.801, pb0.05). Treatment with either L. acidophilus (group III) or olsalazine (group IV) resulted in significant reduction in serumlevels of CRP, TNF-α and IL-6, as well as disease activity index (DAI). Treatment with combination of L. acidophilus and olsalazine (group V) offered more significant reduction in serum levels of CRP, TNF-α, IL-6 and disease activity index (DAI) when compared to either group II (untreated group), group III (treated with L. acidophilus) or group IV (treated with olsalazine). So, it was concluded that L. acidophilus probiotic could be recommended as adjuvant therapy in combination with olsalazine to achieve more effective treatment for ulcerative colitis. For application in human, this needs to be verified in further clinical studies.

Keywords: *Ulcerative colitis; Probiotics; Lactobacillus acidophilus; Olsalazine*